PREDICTION OF AFFLUX AT BRIDGE CONSTRICTIONS USING A DEPTH AVERAGED NUMERICAL MODEL

Mohammad Reza Hadian[(1)], Amir Reza Zarrati[(2)]

[(1)]Assistant Professor, Department of Civil Engineering, Yazd University, Safaiyeh, Yazd, Iran
phone: +98 0351 8211671; fax: +98 0351 8210699; e-mail: mr_hadian@yazduni.ac.ir
[(2)] Associate Professor, Dept. of Civil Eng., Amirkabir University of Technology, 424, Hafez Ave., Tehran, Iran
phone: +98 021 64543002; fax: +98 021 66414213; e-mail: zarrati@aut.ac.ir

ABSTRACT

Calculation of afflux and backwater at bridge constrictions is one of the most important factors which should be considered in hydraulic design of bridges over rivers. The 2D depth averaged form of shallow water equations is employed in the present study to calculate backwater upstream of a constriction. The equations are solved on unstructured blocks with structured grids used in each block. The model uses collocated grid arrangement and SIMPLEC like algorithm for velocity-water surface coupling. As a benchmark, a bridge constriction was simulated in a laboratory flume and was tested for common range of Froude numbers in engineering projects. The water surface profiles were measured at center line of the channel and some cross sections upstream of the constriction and were compared with the results of the numerical model. The comparison showed that both zero equation and k-ε turbulence models which are implemented in the numerical model give accurate results in all Froude numbers tested. It is also shown that the numerical model is more accurate than the empirical method used even though the tests were conducted in a simple straight channel with vertical abutments.

Keywords: afflux, bridge constriction, shallow water, numerical model, depth averaged.

1 INTRODUCTION

Bridges across waterways are grade separation structures like those built to carry traffic over or under other highways. The important difference is that there is an interaction between the river and bridge structure which should be considered in the bridge design. Hydraulic design of bridges can be carried out by an engineer, which is trained in hydraulics, hydrology and river behavior.

An important consideration in the hydraulic analysis of a proposed bridge crossing is the amount of afflux and backwater which may occur by constricting the flow with the highway crossing. Backwater can cause flooding upstream of the constriction and hamper the usage of the highway.

Different methods can be employed in afflux prediction. The simplest method is empirical equations derived by simplifying the classical hydraulic equations and applying some coefficients to make them applicable for these sorts of calculations. There are many tables and graphs to determine such coefficient which are found by experiment in laboratory channels. Among different methods those presented by Chow (1959) and Bradley (1973) can be mentioned here. However, because of many factors that can affect the afflux at a bridge constriction, these equations and graphs are limited to cases which they are determined for. With the rapid progress of computer science and technology, equations of motion can be solved for any bridge crossing to determine afflux and backwater. In the present study the 2D shallow water equations are used for this purpose.

In the present paper, details of the numerical model are briefly reviewed. Then the experimental setup and measurements are explained. The results of the model are then compared with experimental data and empirical method of Bradley (1973).

2 NUMERICAL MODEL

2.1 GOVERNING EQUATIONS

Conservative form of shallow water equations in general curvilinear coordinate system is used in the present study to give the model the flexibility of dealing with complex geometries. Neglecting wind shear stress, Coriolis acceleration, using Boussinesq approximation for Reynolds stresses and applying partial transformation for mapping from Cartesian to curvilinear coordinate with Cartesian velocities as primary variables, the equations will be as (Hadian and Zarrati, 2005):

$$\frac{\partial \zeta}{\partial t}+\frac{1}{J}\left(\frac{\partial}{\partial \xi}(Uh)+\frac{\partial}{\partial \eta}(Vh)\right)=0 \tag{1}$$

$$J\frac{\partial}{\partial t}(h\varphi)+\frac{\partial}{\partial \xi}(hU\varphi)+\frac{\partial}{\partial \eta}(hV\varphi)=\frac{\partial}{\partial \xi}\left(\frac{\Gamma g_{22}}{J}\frac{\partial(h\varphi)}{\partial \xi}\right)+\frac{\partial}{\partial \eta}\left(\frac{\Gamma g_{11}}{J}\frac{\partial(h\varphi)}{\partial \eta}\right)+S_{\varphi} \tag{2}$$

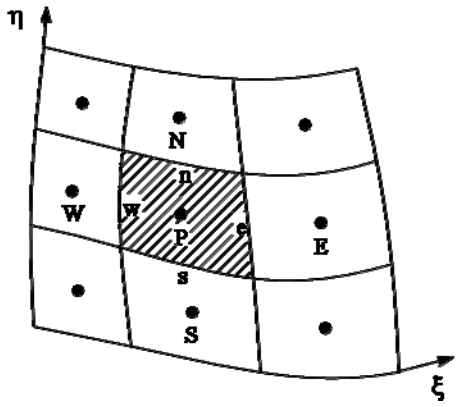

Figure 1. Schematic control volume and notation.

In which, U and V are depth averaged contravariant velocity components in general curvilinear ξ and η directions respectively (Figure 1), φ is transport parameter such as U and V, h= water depth, ρ=water density, Γ= depth averaged viscosity which is equal to v_e for momentum equations and equal to v_e/σ_{φ} for any other φ transported parameters. v_e= depth averaged effective viscosity ($v_e = v + v_t$), v= kinematic viscosity of fluid, v_t= depth averaged turbulent viscosity, g=gravitational acceleration, ζ=water surface elevation ($\zeta = h + Z_b$), Z_b=bed elevation, J= jacobian of transformation ($J = x_{\xi}y_{\eta} - x_{\eta}y_{\xi}$) where x_{ξ}, x_{η}, y_{ξ} and y_{η} are metrics, τ_{bx} and τ_{by}=bed shear stresses in x and y directions which can be calculated using Manning's equation as:

$$\frac{\tau_{bx}}{\rho}=\frac{g n^2 u\sqrt{u^2+v^2}}{h^{\frac{1}{3}}} \tag{3}$$

$$\frac{\tau_{by}}{\rho}=\frac{g n^2 v\sqrt{u^2+v^2}}{h^{\frac{1}{3}}} \tag{4}$$

where u and v are depth averaged Cartesian velocities. The depth averaged contravariant

velocity components, which are tangential to curvilinear coordinate ξ and η respectively, are defined as:

$$U = uy_\eta - vx_\eta \ , \ V = vx_\xi - uy_\xi \tag{5}$$

Other parameters are defined as below:

$$g_{22} = x_\eta^2 + y_\eta^2 \ , \ g_{12} = x_\xi x_\eta + y_\xi y_\eta \ , \ g_{11} = x_\xi^2 + y_\xi^2 \tag{6}$$

$$\begin{aligned} S_U = & -gh\left(y_\eta \frac{\partial \zeta}{\partial \xi} - y_\xi \frac{\partial \zeta}{\partial \eta} \right) - J \frac{\tau_{bx}}{\rho} + \frac{\partial}{\partial \xi}\left[\frac{v_e}{J}\left(y_\eta \frac{\partial (Uh)}{\partial \xi} - y_\xi \frac{\partial (Uh)}{\partial \eta} - g_{12} \frac{\partial (hu)}{\partial \eta} \right) \right] \\ & + \frac{\partial}{\partial \eta}\left[\frac{v_e}{J}\left(y_\eta \frac{\partial (Vh)}{\partial \xi} - y_\xi \frac{\partial (Vh)}{\partial \eta} - g_{12} \frac{\partial (hu)}{\partial \xi} \right) \right] \end{aligned} \tag{7}$$

$$\begin{aligned} S_V = & -gh\left(x_\xi \frac{\partial \zeta}{\partial \eta} - x_\eta \frac{\partial \zeta}{\partial \xi} \right) - J \frac{\tau_{by}}{\rho} \frac{\partial}{\partial \xi}\left[\frac{v_e}{J}\left(-x_\eta \frac{\partial (Uh)}{\partial \xi} + x_\xi \frac{\partial (Uh)}{\partial \eta} - g_{12} \frac{\partial (hv)}{\partial \eta} \right) \right] \\ & + \frac{\partial}{\partial \eta}\left[\frac{v_e}{J}\left(-x_\eta \frac{\partial (Vh)}{\partial \xi} + x_\xi \frac{\partial (Vh)}{\partial \eta} - g_{12} \frac{\partial (hv)}{\partial \xi} \right) \right] \end{aligned} \tag{8}$$

The depth averaged turbulent viscosity can be considered as a constant value, calculated by a zero-equation models or more advanced models like depth-averaged *k-ε*. Here the zero equation model of Jia and Wang (1999) and depth-averaged *k-ε* model are used. The former can be written as:

$$v_t = \frac{\kappa}{6} u_* h \tag{9}$$

In which u_* = bed shear velocity and κ is the von Karman constant (=0.4).

In depth averaged *k-ε* model v_t is calculated as (Rastogi and Rodi, 1978):

$$v_t = C_\mu \frac{k^2}{\varepsilon} \tag{10}$$

The equations of *k* and *ε* can be expressed in general form of transport equations (2) when *φ* is substituted by *k* or *ε* and with using the following source terms:

$$S_k = J(G + P_k - \varepsilon h) - \left\{ \frac{\partial}{\partial \xi}\left(\frac{v_t}{\sigma_k} \frac{g_{12}}{J} \frac{\partial (hk)}{\partial \eta} \right) + \frac{\partial}{\partial \eta}\left(\frac{v_t}{\sigma_k} \frac{g_{12}}{J} \frac{\partial (hk)}{\partial \xi} \right) \right\} \tag{11}$$

$$S_\varepsilon = J\left(C_{1\varepsilon} G \frac{\varepsilon}{k} + P_\varepsilon - C_{2\varepsilon} h \frac{\varepsilon^2}{\bar{k}} \right) - \left\{ \frac{\partial}{\partial \xi}\left(\frac{v_t}{\sigma_\varepsilon} \frac{g_{12}}{J} \frac{\partial (h\varepsilon)}{\partial \eta} \right) + \frac{\partial}{\partial \eta}\left(\frac{v_t}{\sigma_\varepsilon} \frac{g_{12}}{J} \frac{\partial (h\varepsilon)}{\partial \xi} \right) \right\} \tag{12}$$

$$G = \frac{v_t}{h}\left\{ 2T_1^2 + 2T_2^2 + T_3^2 \right\} \tag{13}$$

$$T_1 = \frac{1}{J}\left(y_\eta \frac{\partial (uh)}{\partial \xi} - y_\xi \frac{\partial (uh)}{\partial \eta} \right) \tag{14}$$

$$T_2 = \frac{1}{J}\left(- x_\eta \frac{\partial (vh)}{\partial \xi} + x_\xi \frac{\partial (vh)}{\partial \eta} \right) \tag{15}$$

$$T_3 = \frac{1}{J}\left(- x_\eta \frac{\partial (uh)}{\partial \xi} + x_\xi \frac{\partial (uh)}{\partial \eta} + y_\eta \frac{\partial (vh)}{\partial \xi} - y_\xi \frac{\partial (vh)}{\partial \eta} \right) \tag{16}$$

$$P_k = \frac{u_*^3}{\sqrt{c_f}} \tag{17}$$

$$P_\varepsilon = C_\varepsilon \frac{u_*^4}{h} \tag{18}$$

Other coefficients of *k-ε* equations are tabulated in Table 1(Launder and Spalding, 1974).

Table 1. constant coefficients of *k-ε* equations.

C_μ	$C_{1\varepsilon}$	$C_{2\varepsilon}$	σ_k	σ_ε
0.09	1.43	1.92	1	1.3

2.2 SOLUTION ALGORITHM

The equations are solved on structured grid using control volume method in which the equations are integrated on control volumes (cells) in time and space. (Versteeg and Malalasekera, 1995). Applying Gauss diversion method to convert surface integrals to boundary integrals and the first-order implicit Euler method for time integration, the momentum equations are discretized in the form of:

$$A_P \varphi_P = A_E \varphi_E + A_W \varphi_W + A_N \varphi_N + A_S \varphi_S + A_p^o \varphi_p^o + S_\varphi \tag{19}$$

In which the A_i s are coefficients and the indices are defined considering Figure 1. These coefficients depend on the applied method for discretizing convection-diffusion terms. Here the Power-law scheme is used in numerical model. The east and west factors for power-law schemes can be calculated as:

$$A_E = D_e \max\left(0, \left[1 - \frac{0.1|F_e|}{D_e} \right]^5 \right) + \max(-F_e, 0) \tag{20}$$

$$A_W = D_w \max\left(0, \left[1 - \frac{0.1|F_w|}{D_w} \right]^5 \right) + \max(F_w, 0) \tag{21}$$

$$F_e = (hU)_e \Delta\eta \ , \ F_w = (hU)_w \Delta\eta \tag{22}$$

$$D_e = \left(\frac{\Gamma g_{22} h}{J \Delta\xi} \right)_e \Delta\eta \ , \ D_w = \left(\frac{\Gamma g_{22} h}{J \Delta\xi} \right)_w \Delta\eta \tag{23}$$

and finally:

$$A_P = A_p^o + A_E + A_W + A_N + A_S - S_\varphi^p - \overbrace{(F_e - F_w + F_n - F_s)}^{\Delta F} \tag{24}$$

$$A_p^o = J h_p^o \frac{1}{\Delta t} \Delta\xi \, \Delta\eta \tag{25}$$

where the superscript "^{o}" denotes the values at previous time step.

For better convergence of equations the under-relaxation factors are used by replacing equation (19) with:

$$\frac{A_P}{\alpha_\varphi}\varphi_P = A_E\varphi_E + A_W\varphi_W + A_N\varphi_N + A_S\varphi_S + S_\varphi + A_p^o\,\varphi_p^o + \frac{1-\alpha_\varphi}{\alpha_\varphi}A_P\varphi_p^{**} \tag{26}$$

In the above equation the "**" superscript denotes the values of last iteration.

In which α_φ is the under-relaxation factor for equation of φ.

The water surface is calculated by a SIMPLEC like algorithm following Zhou (1995) and Weerakoon et al. (2003), which was developed for non-orthogonal curvilinear coordinate system by Hadian and Zarrati (2005). Therefore the corrections of contravariant velocities are calculated as:

$$U' = -B\frac{\partial\zeta'}{\partial\xi}\ ,\ B = \frac{g\,h\,\Delta\xi\,\Delta\eta}{\frac{A_p}{\alpha_v} - \sum A_{nb}}\,g_{22} \tag{27}$$

$$V' = -C\frac{\partial\zeta'}{\partial\eta}\ ,\ C = \frac{g\,h\,\Delta\xi\,\Delta\eta}{\frac{A_p}{\alpha_v} - \sum A_{nb}}\,g_{11} \tag{28}$$

The corrections of water surface elevation are calculated by solving the following convection-diffusion type equations:

$$J\frac{\partial\zeta'}{\partial t} + \frac{\partial}{\partial\xi}\left(U^*\zeta'\right) + \frac{\partial}{\partial\eta}\left(V^*\zeta'\right) = \frac{\partial}{\partial\xi}\left(Bh^*\frac{\partial\zeta'}{\partial\xi}\right) + \frac{\partial}{\partial\eta}\left(Ch^*\frac{\partial\zeta'}{\partial\eta}\right) - m \tag{29}$$

$$m = J\frac{\partial\zeta^*}{\partial t} + \frac{\partial}{\partial\xi}\left(U^*h^*\right) + \frac{\partial}{\partial\eta}\left(V^*h^*\right) \tag{30}$$

Though curvilinear coordinate system is a robust tool to handle complex geometry domains, it results in a very skewed mesh in some regions when the flow domain is very complex as it is in the case of bridge constriction. The multi-block technique is one of the most powerful methods which can solve this problem. Here the method of halo cells is used (Lien et al,, 1996; Apsley and Hu, 2003; Hadian and Zarrati, 2005) and the equations are solved in unstructured blocks with one layer thick halo cells.

For the sake of simplicity in programming and especially for implementing the multi-block method, collocated grid has been used, so all the variables are stored at cell centers. To avoid the checkerboard water surface fluctuation, it is necessary to use momentum interpolation method for calculation of contravariant velocities at cell faces in solution of equation (29) and coefficients of transport equation (2). In the present study the method of Lien and Leschziner (1994) was developed for shallow water equations (Hadian and Zarrati, 2006).

In the test cases of present study the flow is sub-critical in both inlet and outlet. So, the water surface elevation is used at outlet as boundary condition while the discharge is introduced at inlet. The wall function method is used at solid walls to bridge the boundary layer and the necessary source terms are added to the equations (Versteeg and Malalasekera, 1995).

At the beginning of calculation, the water surface level at the outlet section was used for all the flow domain as initial condition and velocity in the flow domain was calculated using known discharge and water surface level.

The procedure for solution of equations at every time step can be summarized as follows:

1. Solve the momentum equations for all blocks assuming fixed velocities at halo cells

(frozen halo cells) in each block and then update the velocities in the entire flow domain including in halo cells.
2. Solve the depth correction equation (29) for all blocks using frozen halo cells and then update ζ' in halo cells.
3. Correct the water surface elevation, water depth and all velocities at all blocks.
4. Calculate eddy viscosity by Equation (9) or by solving k-ε equations at every block and update the halo cells.
5. Considering the inlet discharge correct the velocities at inlet section.
6. Repeat the above steps till convergence is achieved.
7. Go to the next time step.

3 EXPERIMENTAL SETUP

The experiments were conducted in hydraulic laboratory of Amirkabir University of Technology. The experimental flume was 6 m long, 0.513 m wide and 0.75 m deep and fed with 2 centrifugal pumps. The bottom of flume was made of painted steel and walls were Perspex material. The bridge constriction was simulated by 2 abutments with length of 10 cm and thickness of 4.2 cm, made up of painted wood. By installing these abutments the bridge opening ratio of 39% was formed in the flume. Water pumped into an inlet tank and flowed into flume after passing some screens that produced almost uniform flow across the channel width. There was a tailgate at the end of the flume which was used to adjust the downstream tail water depth (Figure 2).

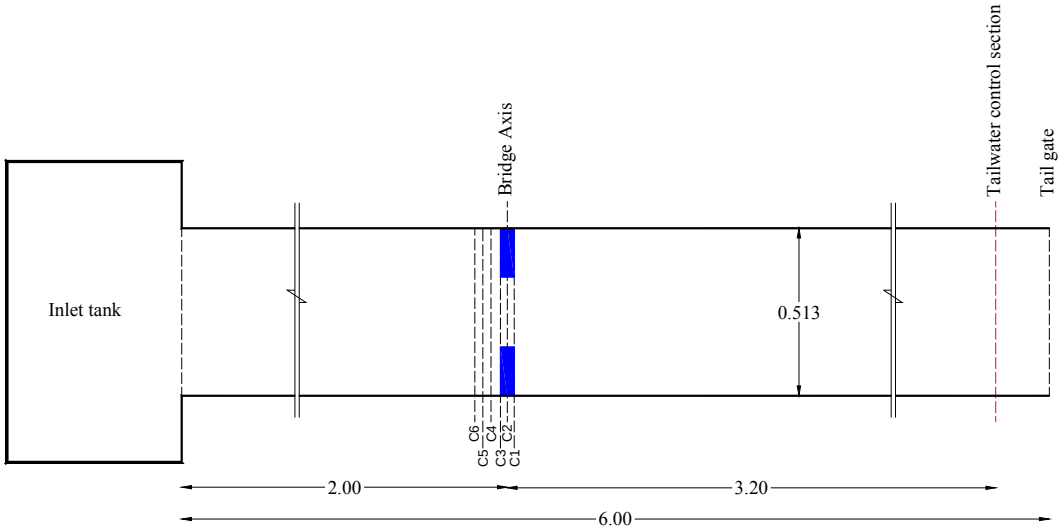

Figure 2. Layout of the experimental flume and transverse sections position.

Experiments were performed for 6 cases with different flow discharge and tail waters as it is summarized in Table 2. With discharges and depths selected, the range of Froude number was between 0.15 to 0.3 similar to mild slope rivers. Figure 3 shows flow condition at the constriction in one of these cases.

Table 2. Main parameters in the experiments.

Test No	T1	T2	T3	T4	T5	T6
Discharge (lit/s)	10	10	15	15	20	20
Downstream tail depth (cm)	10	12	10	12	12	15

Figure 3. Flow at constriction with Discharge=15 lit/s and tail water =12 cm ((view looking upstream).

4 RESULTS AND COMPARISONS

To reduce the CPU time, only half of the channel was modeled and the symmetric condition was applied at the channel axis. As it is presented in Figure 4, five blocks was used to generate the mesh in the flow domain.

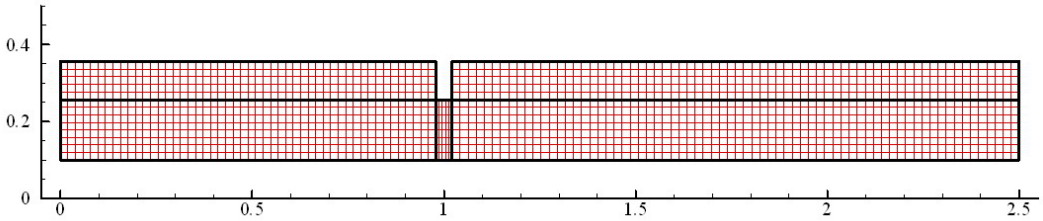

Figure 4. Mesh applied in numerical model.

The water surface profile along the centerline of channel is presented in Figure 5 for different test cases. As the figure shows, the model could predict accurately the water surface location at the upstream side of the bridge. Both the zero equation and k-ε model could predict the water surface elevations with almost the same accuracy. Downstream of the constriction, the pressure distribution deviates from hydrostatic and the results of the shallow water model deteriorate. Deviation from experimental results downstream of the constriction is less in lower values of afflux.

Figure 6 shows water surface profile at transverse sections C1 to C6 (Figure 2) for the test with discharge of 15 lit/s and tail water level of 10 cm. Predictions of the numerical model is very good except at section C1 which is the downstream edge of the abutment where pressures deviate from hydrostatic distribution (Figure 3). It should be mentioned here that empirical relations are unable to give these details on transverse distribution of afflux upstream of the constriction

The empirical method of Bradley (1973) was used here for calculation of afflux in the 6 test cases and its results are compared with the numerical model. The results are presented in Figure 7. In this figure the error in calculating afflux normalized by the tail water depth is plotted verses Froude number. As the figure shows, the accuracy of the present model is much better than the empirical equation especially at higher Froude numbers. Accuracy of both zero equation and *k-ε* model is almost the same, although zero equation model is much simpler. While the error of empirical equation increases with Froude number, the numerical model

error is similar in the range of Froude number tested.

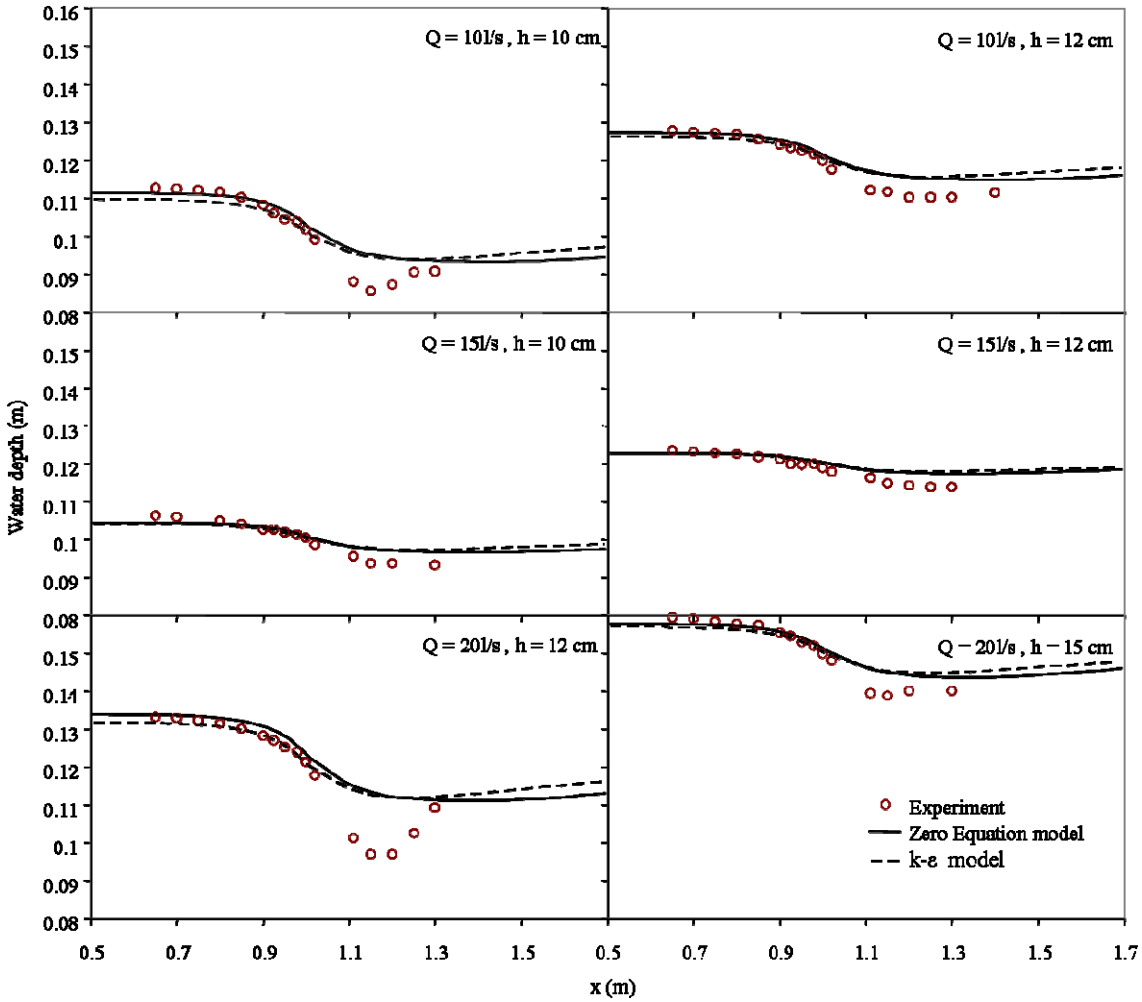

Figure 5. Comparison of water surface profile along channel axis.

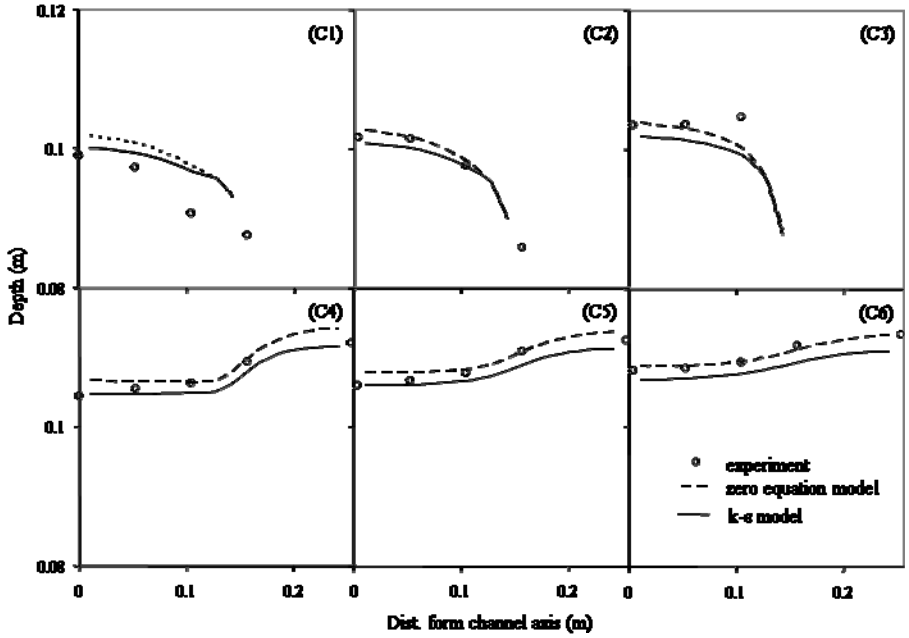

Figure 6. water surface profile at transverse sections.

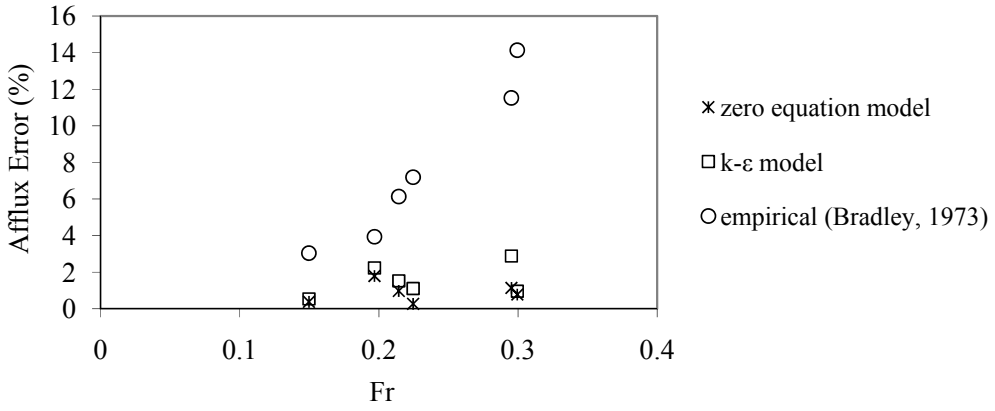

Figure 7.Error in afflux calculation vs. Froude number.

5 CONCLUSIONS

A numerical model based on shallow water equations is developed in the present study to simulate afflux upstream of constrictions. The model solves the transformed equation to general curvilinear coordinate system by control volume method on unstructured Multi-Block grids and structured grid in each block. Halo cell technique is used for data transformation and collocated grids are applied to store the variables. The water surface is calculated using a SIMPLEC like algorithm and both the zero equation and depth averaged k-ε model are implemented for calculating turbulent eddy viscosity. Some experiments were carried out for vertical abutments in a straight channel and water surface profiles were measured along center line of the channel and some cross sections upstream of the constriction.

The model could predict the afflux accurately in all the test cases. The accuracy of the model with k-ε and zero equation turbulence models was similar. Comparison of the present model and empirical method of Bradley (1973) showed that the present numerical model is more accurate even in the simple geometry used in the experiments which these equations were derived for. Moreover, the numerical model gives more details about water surface profiles in transverse direction upstream of the constriction. The accuracy of empirical equations decreased as the Froude number increased however the error of the numerical model was almost similar for different Froude numbers.

ACKNOWLEDGMENTS

The authors would like to appreciate Dr. David Apsley's comments during development of the numerical model. Also, for experimental setup and measurements, kindly assist of Mr. Karimi from the hydraulic laboratory of Amirkabir University of Technology is acknowledged.

REFERENCES

Apsley, D. and Hu,W. (2003), CFD Simulation of Two- and three-Dimensional Free Surface Flow , *International Journal of Numerical Methods in Fluids*, 42, pp. 465-491.

Bradley, J.N. (1973), Hydraulics of bridge waterways (Hydraulic design series), U.S. Federal Highway Administration.

Choi, S.K. (1999), Note on the Use of Momentum Interpolation Method for Unsteady Flows, *Numerical Heat Transfer, Part A*, 36, pp. 545-550.

Chow, V.T. (1959), Open-Channel Hydraulics, McGraw-Hill Book Company.

Hadian, M.R. and Zarrati, A.R. (2005), Simulation of Shallow Flows in a Circular Basin Using Collocated Multi-Block Method, *in Proceedings of XXXI IAHR Congress*, Seoul,

Korea.
Hadian, M.R. and Zarrati, A.R. (2006), Study on the Effect of Momentum Interpolation Method for Solving Shallow Water Equations, *Amirkabir Journal of Science and Technology*, Vol.16, No.63- C(CMM), pp. 31-41 (in Persian).
Jia, Y. and Wang, S.S.Y. (1999), Numerical Model for Channel Flow and Morphological Channel Studies, *Journal of Hydraulic Engineering, ASCE*, 125(9), pp. 924-933.
Lien, F.S. and Leschziner, M.A. (1994), "A General Non-Orthogonal Collocated Finite Volume Algorithm for Turbulent Flow at all Speeds Incorporating Second-Moment Turbulence-Transport Closure, Part 1: Computational Implementation", *Computer Methods in Applied Mechanics and Engineering*, 114, pp. 123-148.
Lien, F.S., Chen, W.L. and Leschziner,M.A. (1996). A Multiblock Implementation of Non-Orthogonal Collocated Finite Volume Algorithm for Complex Turbulent Flows, *International Journal for Numerical Methods in Fluids*, 23, pp. 567-588.
Majumdar,S., (1988), Role of Underrelaxation in Momentum Interpolation for Calculation of Flow with Nonstaggered Grids, *Numerical Heat Transfer*, 13, pp. 125-132.
Miller, T.F. and Schmidt, F.W. (1988), Use of Pressure-Weighted Interpolation Method for the Solution of the Incopressible Navier-Stokes Equations on a Nonstaggered Grid System, *Numerical Heat Transfer*, 14, pp. 213-233.
Rastogi, A,K. and Rodi, W. (1978), Prediction of Heat and Mass Transfer in Open Channels, *Journal of Hydraulics Division, ASCE*, 104(3), pp. 397-420.
Rhie,C.M. and Chow,W.L. (1983), Numerical Study of the Turbulent Flow Past an Airfoil Trailing Edge Separation, *AIAA Journal*, 21(11), pp. 1525-1532.
Yu, B., Kawaguchi, Y., Tao, W.Q. and Ozoe, H. (2002a), Checkerboard Pressure Predictions Due to the Underrelaxation Factor and Time Step Size for a NonStaggered Grid with Momentum interpolation Method, *Numerical Heat Transfer, Part B*, 41, pp. 85-94.
Yu, B., Tao, W.Q., Wei, J.J., Kawaguchi, Y., Toshio, T. and Ozoe, H. (2002b), Discussion on Momentum Interpolation Method for Collocated Grids of Incompressible Flow, *Numerical Heat Transfer, Part B*, 42, pp. 141-166.
Versteeg, H.K. and Malalasekera, W. (1995), An Introduction to Computational Fluid Dynamics, The Finite Volume Method, Longman Book Publisher.
Wang,Y. and Komori, S. (1999), Comparison of Using Cartesian and Covariant Velocity Components on Non-orthogonal Collocated Grids, *International Journal for Numerical methods in Fluids*, 31, pp. 1265-1280.
Weerakoon, S.B., Tamai N. and Kawahara Y. (2003), Flow Computation at a River Confluences, *Journal of Water and Maritime Engineering, Inst. of Civil Engineers*, 1, pp. 73-83.
Zhou, Jian Guo (1995), Velocity-Depth Coupling in Shallow-Water Flows, *Journal of Hydraulic Engineering, ASCE*, 121(10), pp. 717-724.